

Novel Surface-Mounted Neutron Generator

Juan M. Elizondo-Decanini, David Schmale, Mike Cich, Marino Martinez, Kevin Youngman, Matt Senkow, Scott Kiff, John Steele, Ron Goeke, Brian Wroblewski, John Desko, and Alexander J. Dragt

Abstract—A deuterium–tritium base reaction pulsed neutron generator packaged in a flat computer chip shape of 1.54 cm (0.600 in) wide by 3.175 cm (1.25 in) long and 0.3 cm (0.120 in) thick has been successfully demonstrated to produce 10^3 neutrons per pulse (14 MeV) in a 0.5- μ s pulse. The neutron generator is based on a deuterium ion beam accelerated to impact a tritium-loaded target. The accelerating voltage is in the 15- to 20-kV range with a 3-mm (0.120 in) gap, and the ion beam is shaped by using a lens design to produce a flat ion beam that conforms to the flat rectangular target. The ion source is a simple surface-mounted deuterium-filled titanium film with a fused gap that operates at a current–voltage design to release the deuterium during a pulse-length of about 1 μ s. We present some of the preliminary results and the general description of the working prototypes, which we have labeled the “NEUTRISTOR.”

Index Terms—Cancer, commercial, high voltage, ion source, medical, neutron generator.

I. INTRODUCTION

NEUTRON generators that are based on accelerating a deuterium ion beam and impacting a tritium (or deuterium)-loaded target are typically made in a cylindrical shape or symmetry. Cylindrical symmetry allows practical control of the ion beam and the high voltage, and it allows control of ion-induced secondary electrons with a simple structure. The cylindrical package allows for robust and simple structures, particularly for applications such as well logging [1], [2]. What is called “diode” geometry consists of an ion source, an aperture plate with a pin hole in the center or a screen in some designs, an accelerating gap where the ions are accelerated, and a target. The ion source can take several forms, the simplest of which is an electrode pair with a spark gap, where the electrodes of the spark gap are loaded with deuterium [3].

Smaller portable systems continue to be based on thin cylindrical pipes with considerable volume. We demonstrated a

millimeter-sized neutron generator, based on taking the flat cross section of the simplest diode-based neutron generator geometry, and designed an ion lens around it so that the ions hit the target in a flat rectangular shape. This paper discusses the overall cross section (including shape and materials), the lens design, the results of the ion beam model, and the output performance of the neutron chip.

A. “NEUTRISTOR” Application, Shape, and Basic Materials

Our goal was to develop a portable low-voltage battery-operated neutron source capable of being mounted on a socket the size of a computer chip. One application of this technology is to put the neutron source, with a moderator, in a package that can be placed close to a cancerous area, allowing a cancer patient to return to his/her home while receiving a low neutron dose over an extended period of time. In boron neutron capture therapy [4]–[6], a slow neutron is absorbed by boron (${}^{10}\text{B}$) or boronated compounds introduced to the cancer cells, releasing ${}^4\text{He}$ and ${}^7\text{Li}$ with a gamma, with the ${}^4\text{He}$ and ${}^7\text{Li}$ causing most of the cell damage [7].

The shape of the neutron generator was based on the ease of fabrication and expense. Production runs of 20 to 30 chips can be made using readily available lithography and metal deposition techniques. The end result meets the goal of developing and mass producing an inexpensive and portable neutron generator that can easily be adapted to a number of critical applications.

An advantageous aspect of the design is that it is made in stacked layers. Each layer has a particular function, allowing different material deposition and film thicknesses. Most importantly, it allows the loading of deuterium on the ion source layer and tritium on the target layer.

Stacking several generators on top of each other prevents high-voltage breakdown between generators when operated in a sequential mode [8], [9].

The numbered items in Fig. 1 show the basic components:

- 1) ceramic substrate where the ion lens and ion source cavity are mounted;
- 2) ceramic half where the target surfaces are deposited;
- 3) ceramic cover plate that seals the plasma cavity and upper lens bias;
- 4) main target surface;
- 5) top/bottom cover and vacuum seal surfaces;
- 6) target high-voltage connector;
- 7) ion source film structure;
- 8) target film connector;
- 9) ion beam lens;
- 10) ceramic cover plate that seals the plasma cavity and lower lens bias.

Manuscript received November 21, 2011; revised March 19, 2012 and May 24, 2012; accepted May 24, 2012. Date of current version September 10, 2012. This work was supported by the LDRD Program.

J. M. Elizondo-Decanini, D. Schmale, M. Cich, M. Martinez, K. Youngman, M. Senkow, S. Kiff, J. Steele, R. Goeke, B. Wroblewski, and J. Desko are with Sandia National Laboratories, Albuquerque, NM 87185 USA (e-mail: jmelizo@sandia.gov; dtscma@sandia.gov; mjcich@sandia.gov; mmarti8@sandia.gov; kyoungm@sandia.gov; mpseko@sandia.gov; skiff@sandia.gov; jtsteel@sandia.gov; rsgoeke@sandia.gov; bwroble@sandia.gov; jsdesko@sandia.gov).

A. J. Dragt is with Honeywell Federal Manufacturing & Technologies—Kansas City Plant, Kirtland Air Force Base, Albuquerque, NM 87185-5250 USA (e-mail: adragt@kcp.com).

Color versions of one or more of the figures in this paper are available online at <http://ieeexplore.ieee.org>.

Digital Object Identifier 10.1109/TPS.2012.2204278

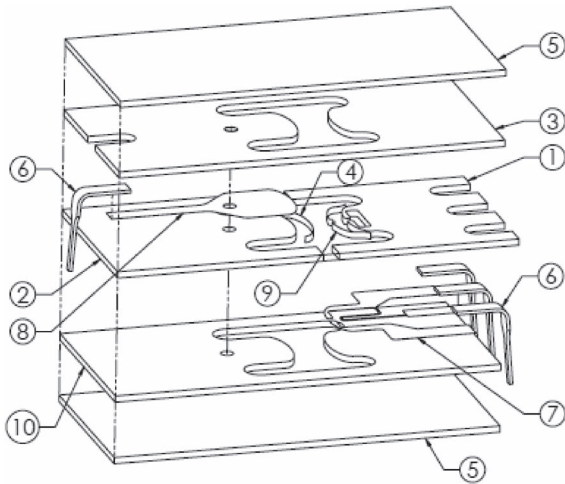


Fig. 1. "NEUTRISTOR" basic shape and components.

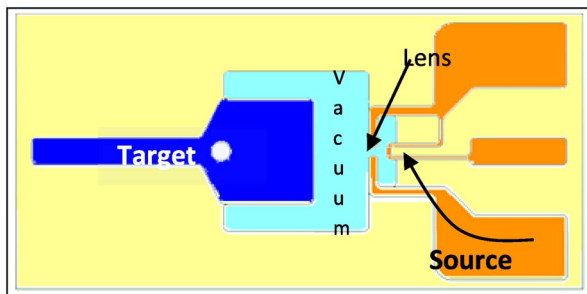


Fig. 2. Surface-mounted generator basic components.

All parts (Fig. 2) are made out of ceramic with metal films vapor-deposited on top by different methods, including lithography and plain mask and evaporator techniques.

The wafer has the following dimensions:

- 1) width: 1.54 cm (0.600 in);
- 2) length: 3.175 cm (1.25 in);
- 3) thickness: 0.05 cm (0.020 in).

The tested units were fabricated with two source wafers. The aspect ratio was defined by the high voltage required in the accelerating cavity and the appropriate electric field management. A minimum of 15 kV was established as the operating accelerating voltage. This is derived from the fact that, at 10-keV ion energies (or less), the probability of deuterium–deuterium (DD) or deuterium–tritium (DT) fusion reaction is at a minimum or nonexistent. The only constraint is to operate the device at the lowest possible voltage—higher voltage will require larger dimensions to keep electric fields within manageable levels. The voltage is then used to determine the neutron yield for DT reactions of thick target technologies [10], which, at 15 kV, is approximately 6×10^4 neutrons/ μC , using 100% loading.

The shape of the accelerating cavity is adjusted after calculating the electric fields at both static and dynamic conditions. Dynamic condition is understood to be when the ion beam and the space charge are present and distributed on the structure. The ion beam accelerating cavity, as designed, was able to take 21 kV with a 10- μs -long pulse and somewhat higher voltage with shorter pulselengths. Most electrostatic models were made using commercially available codes [11].

B. Ion Source

The ion source is based on a simple widely used concept that is described in [3] (see also [12]). It consists of a pair of electrodes facing each other across a gap. In a typical two-electrode spark gap configuration, one electrode is subjected to a sufficiently high voltage until it breaks down, forming an arc through the gap to the second electrode. In this case, the arc is initiated by a vacuum flashover of the ceramic surface between electrodes. The electrodes are made out of a titanium thin film to allow deuterium loading (the details of the gas loading process are beyond the scope of this paper).

In a typical operation and after the current is established, the temperature of the film rises, particularly at the vicinity of the arc, releasing deuterium gas and ionizing it at the same time due to the arc electron flow. The source shape, thickness, and material are designed and selected after a detailed thermal analysis using a commercial multiphysics software package [13].

The temperature profile yields the electrical current drive conditions for the ion source. The required current is determined by knowing the temperature at which deuterium is released from the film at a given thickness. The interelectrode gap was selected following a simple rule of thumb for ceramic flashover: $\sim 50\text{-kV/cm}$ electric field with a field enhancement factor of approximately three, which yields an electric field design value of 150 kV/cm. This value is used to determine the voltage to breakdown and the electrode gap distance. In this case, a gap of about $0.25\text{ }\mu\text{m}$ required an initial voltage of over 1000 V to produce an arc across the electrodes. After the first arc breakdown and due to residue material on the gap, subsequent operations required approximately 300 to 400 V to operate the source.

Next, the ion source was fabricated following a simple design with two electrodes facing each other. As expected, the prototypes worked close to the design value with no gas loaded into the film. The shot life number of the film is very low. With gas loaded, the shot capacity of the source is in 1000 s.

The ion source operation was tested in a simple field-free time-of-flight configuration [14]. The detector is a high-quality Faraday cup [15] capable of bias to suppress secondary electrons and a separate bias to stop ions of lower energy from entering. The deuterium ion source plasma, in a free-expanding mode, can be correlated to the resulting device ion beam current only after both measurements are done and can be analyzed as a function of the ion beam lens extraction, or aperture, efficiency. As an estimate, using the metal vapor arc "rule of thumb" for ion extraction [16] at a conservative level of 1% and estimating (from the thick target yield at 15 kV which is approximately 6×10^4 neutrons/ μC) a neutron production quantum efficiency of $\sim 10^{-8}$ neutrons per ion, it turns out that the plasma current required to produce 2000 neutrons is $\sim 3.3\text{ A}$ for a corresponding $\sim 33\text{-mA}$ ion beam current with a 1- μs -long pulse, matching the results quite closely. Measurements of the ion source plasma, in free expansion, were made, but measurements of the ion beam with either the beam lens or the target present were not performed but will be done; furthermore, their comparison will be reported at a later time.

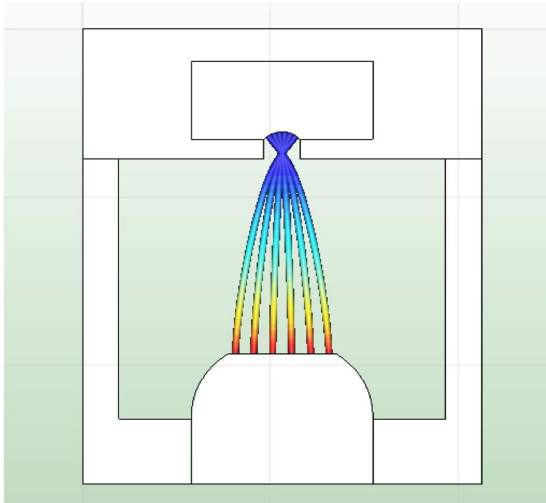


Fig. 3. Model representation of the ion beam expanding on the X -axis.

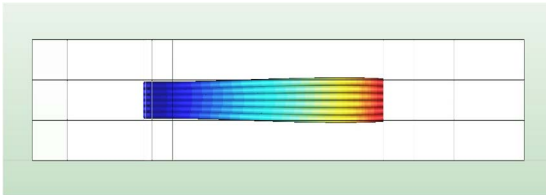


Fig. 4. Model representation of the ion beam expanding on the Y -axis.

C. Target

The target is a film of titanium loaded with tritium. The shape was designed to work in conformity with the ion beam lens. Different shapes are possible, but the elliptical form worked better with the final ion beam lens design. The drivers for the cavity shape were the high voltage and, specifically, the surface flashover. The target was designed with the minimum neutron output required as a guide for the surface area. The thickness can be estimated based on the stopping power of the ion energy at the surface; in this case, we used $2\text{-}\mu\text{m}$ vapor-deposited titanium. No temperature requirements were considered for the design, given that nonrepetitive operation was intended. The target was 100% tritium loaded to enhance the number of tritium clusters available for fusion reaction. The hydride process is performed at about 10^3 Pa and $300\text{ }^\circ\text{C}$ [17], [18].

D. Ion Beam Lens

The initial shape of the ion beam lens was calculated using the paraxial approximation [19]. We determined the approximate lens dimensions to fit our accelerator cavity. Next, we used an elliptical profile to allow the beam to expand to ~ 2 to 3 mm on the X -axis, as shown in Fig. 3, but restricted to $\sim 0.5\text{ mm}$ on the Y -axis, as in Fig. 4.

The general shape of the lens, shown in Fig. 5, is formed by sweeping an elliptical surface across three layers, allowing for an aperture on the center layer for ion extraction.

The resulting electric field distribution shapes the ion beam. Fig. 6 shows the ion beam model with no bias on the lens surfaces where, obviously, the ions (represented by the rays) expand well beyond the target area.

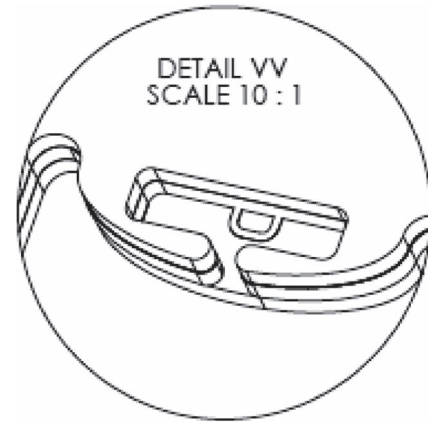


Fig. 5. One elliptical design that is used on the modeling results.

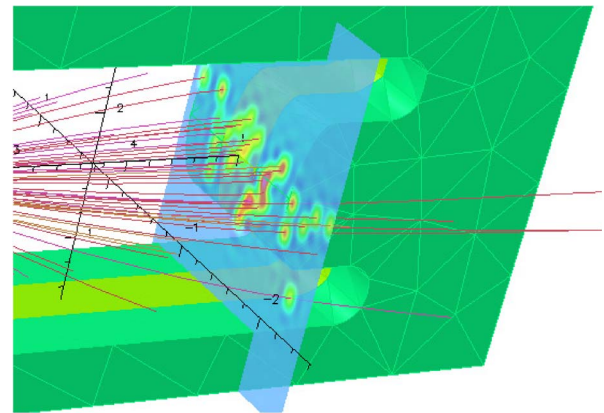


Fig. 6. No bias on the ion beam lens, showing the beam scattered outside the target area.

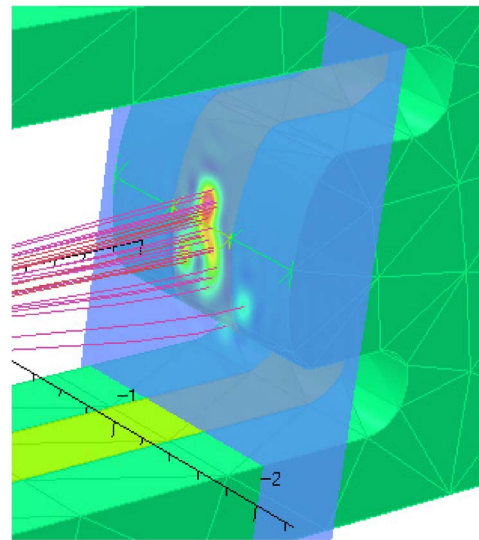


Fig. 7. Fully biased ion beam lens surfaces, showing a better focused beam.

Fig. 7 shows the ion beam trajectories with the surfaces fully biased, where the beam is mostly inside the target area.

The top and bottom surfaces can be modified somewhat. Fig. 7 shows the results using a 3 : 1 (semimajor to semiminor) elliptical ratio on the front surfaces.

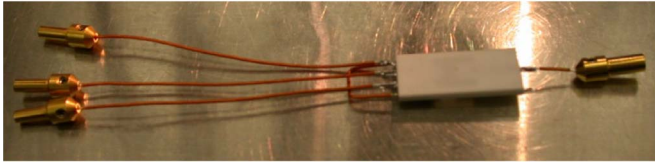


Fig. 8. One sample ready to be inserted into the vacuum test setup. The sample consists of two ion sources and one target. The three cables on the left represent the ground and two current feeds, one for each ion source; the right-hand-side cable is the target high-voltage bias.

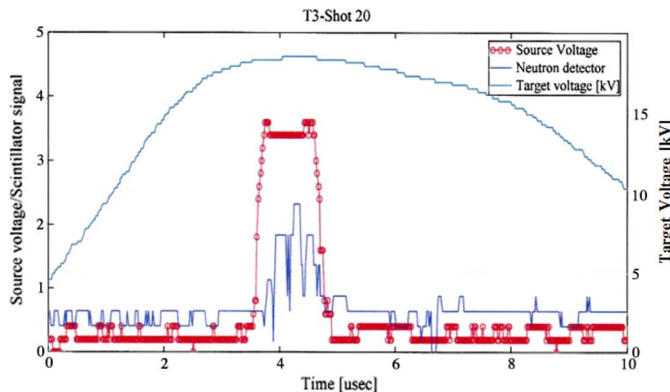


Fig. 9. Voltage, ion source, and neutron detector waveforms for a randomly selected shot. The time scale is 10 μ s. The vertical scales are arbitrary.

Other designs for ion lenses are possible. For instance, we used a flat front target with a two-radius surface on the side of the aperture, resulting in a more focused beam on the target. The ellipse aspect ratio of the semiminor/semimajor axis changes the effective electric field distribution and, therefore, the focal point of the ion beam. We used this information to adjust the length of the cavity, with no changes on the thickness.

E. Experimental Results

Initial testing was done with targets and ion sources unloaded to confirm the levels of high voltage that the chip could accommodate. Next, we tested ion sources loaded with deuterium, with high voltage across the gap, but no tritium on the target. This test confirmed the presence of the ion beam and the high-voltage standoff with the beam in the gap.

Finally, we introduced samples fully loaded with tritium. Because the target is loaded with tritium, the experimental setup was placed in a radiation-controlled area.

The neutron chip target bias is driven with a push-pull circuit that feeds a step-up transformer that produces a 20-kV trapezoid-shaped waveform of about 6- μ s full-width at half-maximum (FWHM). Next, the ion source is turned on at the start of the flat section of the high-voltage pulse, with a 600-V square pulse of about 1- μ s FWHM. The detector is located 2 cm away from the neutron source.

A typical sample tested is shown in Fig. 8. The samples are completely enclosed, and provisions were made in the event that the vacuum equipment became contaminated with tritium.

The target voltage, the ion source pulse, and the neutron detector signal are shown in Figs. 9 and 10. Note that the waveforms have been polarity adjusted for the sake of presentation. Fig. 9 shows the data using a 20-kHz filter on the scope (Tektronix 3054C); Fig. 10 has no filter.

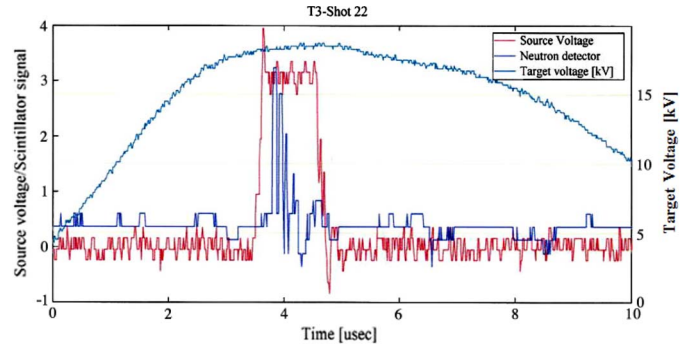


Fig. 10. Voltage, ion source, and neutron detector waveforms for a randomly selected shot. The time scale is 10 μ s. The vertical scales are arbitrary.

The detector used was calibrated using a known DD neutron source. A two-detector setup is used to time correlate the signal. One detector is placed about 2 cm from the source, while the second detector is moved to an equivalent distance to register approximately 2000 neutrons. All measurements were done using a time window that correlated with the application of the ion source pulse.

The detector contains an Eljen EJ309:B5 liquid scintillator as a detection medium [20]. This scintillator contains $\sim 5\%$ B-10 (4.6%), hence the “B5” designation. In our experiments and in published results, the amplitude of thermal neutron captures on B-10 is very small and is likely under the counting threshold of the experiment.

The detector length and diameter are 12.7 cm. There is a small gas bubble in the detector to allow for thermal expansion without damaging the assembly. The photomultiplier is a Hamamatsu H6527.

II. CONCLUSION

We have demonstrated the operation of a simple all-surface-mounted component neutron source. The source size and configuration were selected to fit into a conventional computer chip multilink socket. We have also demonstrated ion beam lens designs that use nonconventional surfaces to produce a flat-shaped ion beam that conforms to the target surface. Outputs in the 2000 neutrons in a 1- μ s-long pulse ($\sim 10^9$ neutrons/s) were measured with a liquid scintillator.

The total ion beam current, or target current, was measured but includes the ion-produced electron secondary emission component. The ion source operation was measured using a free-expansion setup with a Faraday cup; in this setup, we can estimate the D-ion production. The actual ion production, from the ion source, will be measured using a time of flight and reported later, including its correlation to the ion source geometry, thickness, drive current, gap dimensions, and temperature profile.

Measuring neutrons at the level reported was a challenge. We started using a lead probe, in different modes, until we obtained a reasonable signal, but because of noise, we could not say with certainty if it was only due to neutrons. After that, we tested a series of commercial detectors and others available here at Sandia National Laboratories. Finally, the liquid scintillator was made available; time was spent to make sure that the

calibration, noise, X-ray, and gamma discrimination was properly understood and controlled. To confirm the signal discrimination, we used two similar detectors, with a calibrated source, and we moved one detector away until the solid angles were equivalent to capture the minimum signal that we may produce from our device. This probe responded properly to all our shielding and source/no-source testing. The detector measurements correlated well with the estimated neutron output, once we accounted for the proper yield.

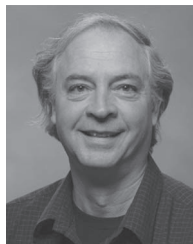
A completely vacuum-sealed self-contained prototype is currently being tested. The process to fully vacuum seal off the unit includes using a preformed package ceramic box with brazed washers. This practical device, which can be used for medical applications, can be made with a DD loading, a source, and a target and may be paired with a boron trifluoride (BF_3) detector [21], [22] for reference measurements.

ACKNOWLEDGMENT

Sandia National Laboratories is a multiprogram laboratory managed and operated by Sandia Corporation, a wholly owned subsidiary of Lockheed Martin Corporation, for the U.S. Department of Energy's National Nuclear Security Administration.

REFERENCES

- [1] E. W. Sengel, "Bill," in *Handbook on Well Logging*. Oklahoma City, OK: Inst. Energy Develop., 1981.
- [2] A. Bourgoyne, K. Millheim, M. Chenevert, and F. S. Young, Jr., *Applied Drilling Engineering*. Richardson, TX: Soc. Petrol. Eng., 1986.
- [3] A. A. Logatchev, "The behavior of vacuum arc discharges on hydrogen impregnated electrodes," *IEEE Trans. Plasma Sci.*, vol. 27, no. 4, pp. 894–900, Aug. 1999.
- [4] G. L. Locher, "Biological effects and therapeutic possibilities of neutrons," *Amer. J. Roentgenol. Radium Therapy*, vol. 36, pp. 1–13, 1936.
- [5] L. E. Farr, W. H. Sweet, J. S. Robertson, C. G. Foster, H. B. Locksley, D. L. Sutherland, M. L. Mendelsohn, and E. E. Stickley, "Neutron capture therapy with boron in the treatment of glioblastoma multiforme," *Amer. J. Roentgenol. Radium Ther. Nucl. Med.*, vol. 71, no. 2, pp. 279–293, 1954.
- [6] M. Suzuki, S. I. Masunaga, Y. Kinashi, M. Takagaki, Y. Sakurai, T. Kobayashi, and K. Ono, "The effects of boron neutron capture therapy on liver tumors and normal hepatocytes in mice," *Jpn. J. Cancer Res.*, vol. 91, no. 10, pp. 1058–1064, Oct. 2000.
- [7] Y. Mishima, *Cancer Neutron Capture Therapy*, Y. Mishima, Ed. New York: Plenum Press, 1996.
- [8] J. M. Elizondo, "Photoconductive semiconductor switch flashover suppression," in *Proc. 14th IEEE Int. Symp. Discharges Elect. Insul. Vac.*, R. Stinnett, Ed., Santa Fe, NM, Sep. 1990.
- [9] J. M. Elizondo, "Novel high voltage vacuum surface flashover insulator technology," in *Proc. 25th Int. Symp. Discharges Elect. Insul. Vac.*, Darmstadt, Germany, Sep. 1992.
- [10] SC-TM-66-247 L. Shope, Theoretical Thick Target Yields for DD, DT, and TD Nuclear Reactions 1966, Jul. SC-TM-66-247.
- [11] Lorentz 2D and 3D, INTEGRATED Engineering Software, Winnipeg, MB, Canada.
- [12] N. Vogel, "The cathode spot plasma in low current air and vacuum break arcs," *J. Phys. D., Appl. Phys.*, vol. 26, no. 10, pp. 1655–1661, Oct. 1993.
- [13] COMSOL Multi-Physics, V4.1.
- [14] I. G. Brown, J. E. Galvin, R. A. MacGill, and R. T. Wright, "Improved time of flight ion charge state diagnostic," *Rev. Sci. Instrum.*, vol. 58, no. 9, pp. 1589–1592, Sep. 1987.
- [15] Kimball-Physics, Faraday Cup Model FC 73-A.
- [16] A. Anders, *Cathodic Arcs*. New York: Springer-Verlag, 2008.
- [17] P. Vajda, "Hydrogen in rare metals, including RH_{2+x} phases," in *Handbook on Physics Chemistry of Rare Earths*, vol. 20. New York: Elsevier Science, 1995, ch. 137.
- [18] J. Bloch and M. H. Mintz, "Kinetics and mechanism of metal hydride formation—A review," *J. Alloys Compounds*, vol. 253/254, pp. 529–541, May 1997.
- [19] S. Humphries, *Principles of Charge Particle Acceleration*. Hoboken, NJ: Wiley, 1999.
- [20] Eljen Technology, Sweetwater, TX.
- [21] D. P. King and L. Goldstein, "The total cross section of the nucleus for slow neutrons," *Phys. Rev.*, vol. 75, no. 9, pp. 1366–1369, May 1949.
- [22] S. Mahmood, S. V. Springham, T. Zhang, R. S. Rawat, T. L. Tan, M. Krishnan, F. N. Beg, S. Lee, H. Schmidt, and P. Lee, "Novel fast-neutron activation counter for high repetition rate measurements," *Rev. Sci. Instrum.*, vol. 77, pp. 10–13, 2006.



Juan M. Elizondo-Decanini received the Ph.D. degree for work on the physics of laser plasmas under high magnetic fields from The University of New Mexico, Albuquerque, in 1987.

For more than ten years, he was the Experimental and Theoretical Physics Group Leader for Tetra Corporation, a pulsed-power high-technology firm in Albuquerque. He has been a Member of the following: 1) the Air Force Research Laboratory, developing microwave-based weapon systems; 2) Honeywell Federal Manufacturing & Technologies—Kansas City Plant, developing compact pulsed-power systems; 3) the Los Alamos National Laboratory Design Team of the Atlas 28 Mega-Ampere (MA) Liner Implosion Machine; and 4) the Sandia National Laboratories (SNL) Design Team of the ZR-Z Pinch 30 MA Accelerator where he designed the water power flow section and the vacuum insulator stack. He is currently a Distinguished Member of the Technical Staff with the Neutron Generator Design, Science and Technology Group, SNL, Albuquerque.

Dr. Elizondo-Decanini was the recipient of the prestigious R&D 100 Award for the development of a laminated insulator (microstack insulator). He was also the recipient of the Individual Technical Excellence Award, one of the SNL employee highest awards for technical achievement.

David Schmale, photograph and biography not available at the time of publication.

Mike Cich, photograph and biography not available at the time of publication.

Marino Martinez, photograph and biography not available at the time of publication.

Kevin Youngman, photograph and biography not available at the time of publication.

Matt Senkow, photograph and biography not available at the time of publication.



Scott Kiff received the B.S. and M.S. degrees in nuclear engineering from Purdue University, West Lafayette, IN, in 2001 and the Ph.D. degree in nuclear engineering from the University of Michigan, Ann Arbor, in 2006.

He was with Pacific Northwest National Laboratory in 2007–2008, where his work included simulations and experimental work supporting development of radiation detection systems for homeland security and nuclear nonproliferation missions. He joined Sandia National Laboratories, Albuquerque, NM, in 2009, where he currently develops radiation detection systems for nuclear safeguards and emergency response applications. Much of this work is focused on fast neutron detection and signatures, although it also includes work on antineutrino detectors to monitor reactor operations for international safeguards.

John Steele, photograph and biography not available at the time of publication.

Ron Goeke, photograph and biography not available at the time of publication.

Brian Wroblewski, photograph and biography not available at the time of publication.

John Desko, photograph and biography not available at the time of publication.



Alexander J. Dragt received the B.S. degree in electrical engineering from The University of New Mexico, Albuquerque.

He has extensive experience in high voltage and pulsed power. He is a Senior Electrical Engineer with Honeywell Federal Manufacturing & Technologies—Kansas City Plant, Kirtland Air Force Base, Albuquerque, where he has worked since 1998. He has coauthored and authored the following papers related to insulator breakdown and Marx generators: *Vacuum Flashover Characteristics*

of Laminated Polystyrene Insulators, with Elizondo-Decanini *et al.*, proceedings of the 12th IEEE International Pulsed Power Conference, and *Compact, Battery-Powered, 400-kV, 40-Joule Marx Generator*, with Elizondo-Decanini, proceedings of the 13th IEEE International Pulsed Power Conference.